Realization of an Ultrastable 578 nm Laser for Yb Lattice Clock

M. Pizzocaro[1,2], G. A. Costanzo[2], A. Godone[1], F. Levi[1], A. Mura[1], and M. Zoppi[1,2], and D. Calonico[1]

[1] INRIM- Optics Division, Torino, Italy.

[2] Politecnico di Torino- Electronic Department, Torino, Italy.

d.calonico@inrim.it

***Abstract*—In this paper we describe the development of an ultrastable laser source at 578 nm, realized with a frequency sum generation. This source will be used to excite the clock transition $^1S_0 \rightarrow {}^3P_0$ in a Ytterbium optical lattice clock experiment. Two independent ultrastable lasers have been realized, and the laser frequency noise and stability have been characterized.**

I. INTRODUCTION

In view of the realization of a Yb optical lattice clock an ultra-stable laser at the wavelength of 578 nm is required. This wavelength corresponds to the $^1S_0 \rightarrow {}^3P_0$ clock transition, whose natural width is ≈10 mHz [1], and unfortunately it is not currently available in semiconductor Fabry-Pérot lasers, neither in fiber lasers devices; at this wavelength, a laser with enough power and narrow linewidth fitting our purposes can't be realized by second harmonic generation from a 1156 distributed feedback (DFB) laser, while it is possible using other, less narrow-linewidth semiconductor laser [2].

The yellow light is generated in a waveguide non-linear crystal by sum frequency of a 1319 nm Nd:YAG laser and a 1030 nm Yb doped fiber laser [3,4]. After the sum generation two ultrastable lasers are obtained starting from the same light source. In our setup two independent Fabry-Pérot cavities are used to stabilize the lasers frequency and we are able to fully characterize

the spectral properties of the low noise lasers. In fact, after the frequency locking loops the correlated part of the noise spectrum of the two lasers is negligible.

II. SUM FREQUENCY GENERATION

The scheme we chose to realize the 578 nm source is reported in Figure 1. The laser radiation is obtained by sum frequency generation of two infrared laser sources (1030 nm and 1319 nm) whose linewidth is of the order of few tens of kHz. A single stage frequency stabilization system is therefore enough to realize an ultra low noise laser source.

The non-linear crystal we use is a waveguide, magnesium-doped, periodically poled lithium niobate (PPLN) device and works in single pass. Infrared light of both lasers is delivered to one of the 32 channels of the crystal through a polarization-maintaining fiber coupler (y-shaped). The output of the fiber device has a bare fiber end, aligned close to the input face of the crystal to couple the light into the waveguide channel (the distance is of the order of 1 μm and not all the channels have the same efficiency). The crystal is placed on a high precision manual 3-axes stage to easily align the fiber with the chosen waveguide. At the crystal output a microscope objective collimates the laser beam, and then the residual infrared light is filtered using mirrors for the visible wavelength.

The output power is maximized tuning the temperature of the crystal. The power of the 578 nm light, as reported in figure 2, shows a diffraction-like behavior around the phase-matching temperature (around 76 °C for our crystal), typical of the non linear frequency sum process in PPLN crystals. We were able to generate up to 12 mW of light at 578 nm.

We measured the short term, relative power instability of the 578 nm light (Fig. 3) since amplitude laser noise can convert to heat noise in the stabilization cavities. The power impinging on each cavity is now 60 μW, and will be reduced and stabilized in the future.

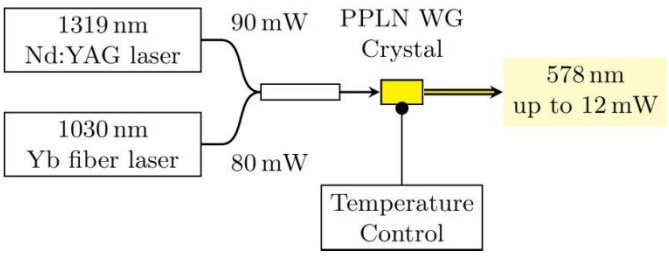

Figure 1. Scheme for Sum Frequency Generation of the 578 nm laser source.

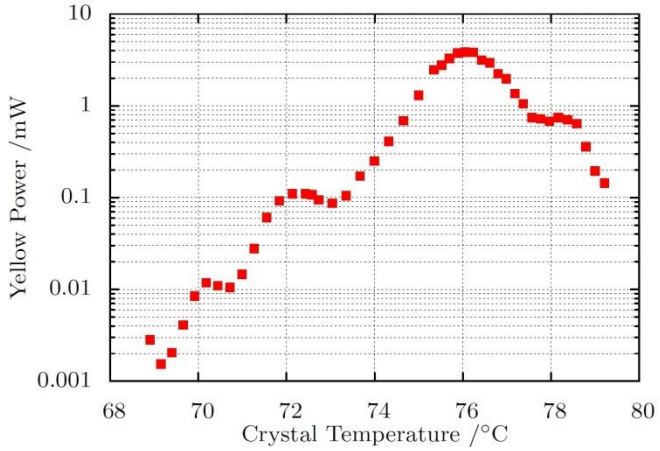

Figure 2. Characterization of the sum frequency generation: output power vs crystal temperature.

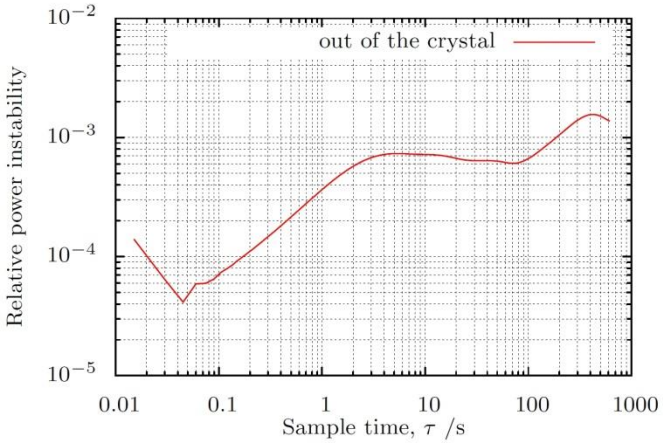

Figure 3. Relative power instability of the 578 nm source.

III. LASER FREQUENCY STABILIZATION

A couple of ultrastable Fabry-Pérot cavities are used as references to independently stabilize the frequency of the clock lasers via the Pound-Drever-Hall (PDH) technique. The two 10 cm long cavities are completely (spacer and mirrors) made of Corning Ultra Low Expansion Glass (ULE), their free spectral range is $\Delta\nu_{FSR}$ = 1.5 GHz and they have respectively a finesse of F_1 = 151000 ± 1000 and F_2 = 224000 ± 4000, as results from cavity ring-down experiments.

The cavities are realized with a notched cylinder and are suspended horizontally, on four points, onto an aluminum structure. Figure 4 shows the artistic drawing of the cavity ensemble with the aluminum support and the copper thermal shield.

Once the PDH locking is properly operated the frequency noise spectrum of the laser closely reproduces that of the reference cavity, so it became of extreme importance to reduce the impact of vibrations that will eventually be converted in laser frequency noise. A proper design and proper suspension of the optical cavity result in a strong attenuation of the vibration sensitivity of the cavity itself, making much easier the design of a compact anti-vibration suspension [5,6].

Aiming to reduce the sensitivity of the cavity resonance frequency to vibrations, we have performed a finite element analysis to investigate the elastic deformation of the Fabry-Pérot cavity under the action of gravity. This static boundary condition is then extrapolated to obtain the vibration sensitivity in the vertical and horizontal directions, hereafter referred to as *xyz* directions.

The final position of the four suspension pads is chosen to minimize the sensitivity of the optical axis length to vertical acceleration (the cavity is said to be supported at the Airy points).

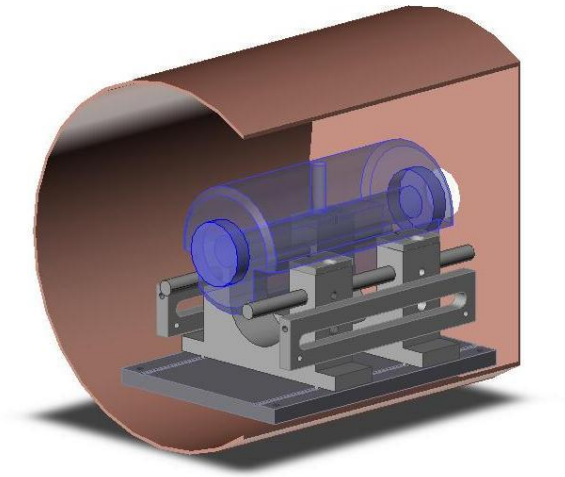

Figure 4. Drawings of the cavity, its supporting structure and the copper thermal shield.

When suspended with the pads at the optimal position not only the optical axis length variation is minimized, but this condition is maintained for relevant displacements from the optical axis on the mirror section. In Figure 5, the vertical sensitivity to vibrations is reported with respect to the vertical displacement from the optical axis and for some possible pads positions. To locate the pads position, we have chosen the distance *m* from the mirror side of the spacer and the distance *n* from the internal

side of the notch. Similar values are obtained for the *x* and *y* direction sensitivities and for horizontal displacement on the mirror. The lower vibration sensitivity is $4\times10^{-11}s^2m^{-1}$ when the pads are located with *m=19* mm and *n=2* mm. As shown, a change in the pads position could result in a large increase of sensitivity even within 1 mm pads displacement along the axial direction.

For a better insulation of the cavity from external world vibrations and temperature fluctuations, each cavity is separately held on top of a passive vibration isolation platform, inside an acoustic shielding enclosure. The cavity is also placed in a thermal copper shield inside a vacuum chamber at the pressure $< 2 \times 10^{-4}$ Pa maintained by a 2 l/s ionic pump.

The residual mechanical noise on top of the vibration isolating platform was measured with a seismometer (Figure 6); as can be observed the platform is quite efficient in reducing the vibration above 1 Hz in the *xyz* directions, allowing on average between 10 and 20 dB of insulation, depending on the Fourier frequency. The finite element analysis shows that the measured residual seismic noise is compatible with an instability in the laser frequency of 1×10^{-15} at 1 s when the cavity is properly suspended at the Airy points.

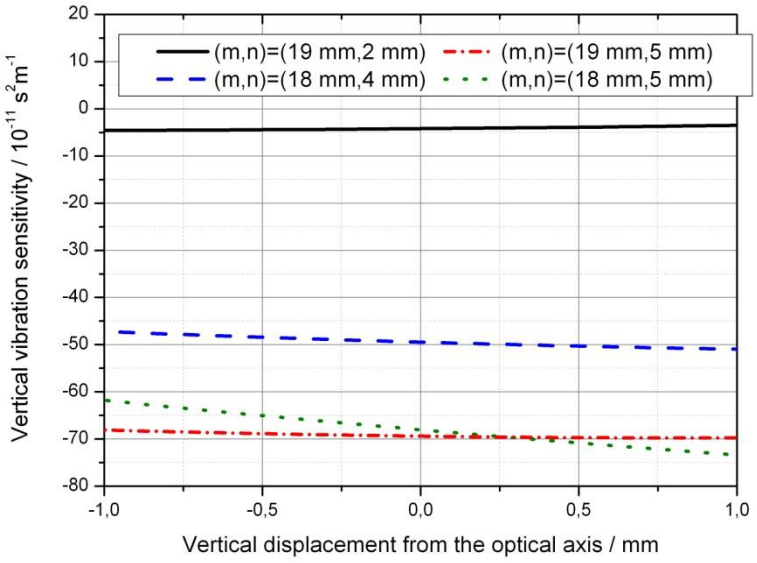

Figure 5. Cavities vertical vibration sensitivity vs the vertical displacement from the optical axis, as simulated by Finite Element Analysis. The sensitivity change for some supports displacements from the optimum is reported. See text for the support location definition.

In view of our spectroscopic application it is not only important to reduce the laser linewidth, but it is also important to guarantee a low frequency drift. Thermal isolation and stabilization is achieved with a copper shield surrounding the cavity inside the vacuum vessel. A digital control stabilizes the temperature of the shield, acting on two heaters external to the vacuum chamber. The ULE cavities have a zero in the coefficient of thermal expansion (CTE) around room temperature. To estimate its value, once locked the two lasers on the two cavities, a linear temperature ramp is applied to the shield of only one of the cavities, keeping the other as reference while monitoring the beat note frequency of the lasers. Aside from an exponential transient and a time lag, the temperature of the cavity itself should vary linearly. This method allows to estimate the zero of the CTE at about 21 °C as reported in Fig. 7; unfortunately this temperature is below the room temperature, and hence it was not yet possible to tune the cavity to this temperature, being the implemented temperature control based only on heating components. However as reported later, the frequency drift in closed temperature loop is low enough to be handled by a compensation for the optical clock realization.

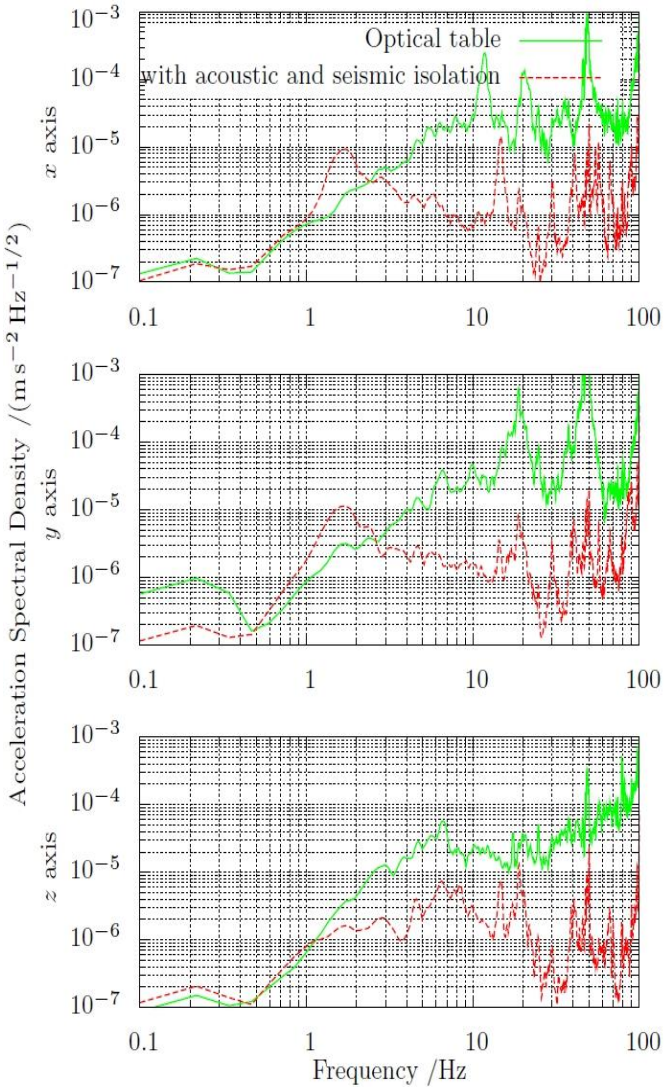

Figure 6. Seismic Noise in the laboratory, on the acustic enclosure floor (upper curves) and on the seismic damping board (lower curves) in the horizontal *x* and *y* and vertical *z* directions: .

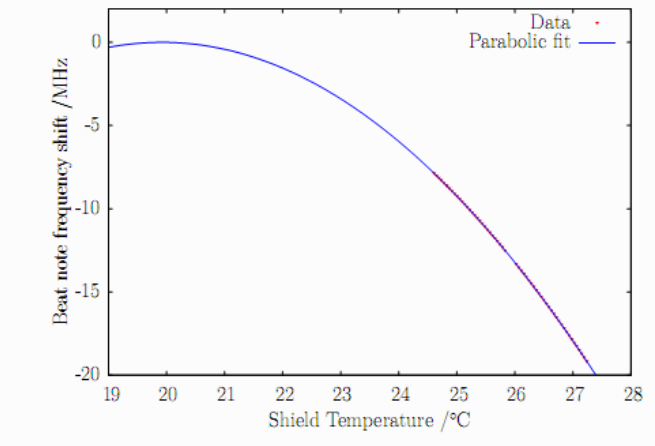

Figure 7. Frequency of the beatnote changing one cavity temperature to measure the cavity zero CTE point.

The Pound-Drever-Hall (PDH) technique is used to stabilize the frequency of the yellow lasers against the resonances of the cavities. As shown in Fig. 8 the 578 nm laser at the output of the crystal is split and delivered to the cavities through polarization-maintaining fibers (about 60 μW of laser are impinging on each cavity).

Two different beams from the same laser are independently frequency stabilized. In both case an electro-optic modulator (EOM) is used to add sidebands to the carrier of the yellow laser (clearly visible in the transmission signal as reported in Figure 8). Thus, an optical circulator/isolator allows to extract the reflected beam and to obtain the PDH error signal.

A double pass acousto-optic modulator (AOM) is used for the fast locking of the laser frequency on each cavity. A proportional-integral-derivative (PID) control is used, while a voltage-controlled oscillator (VCO) drives each AOM.

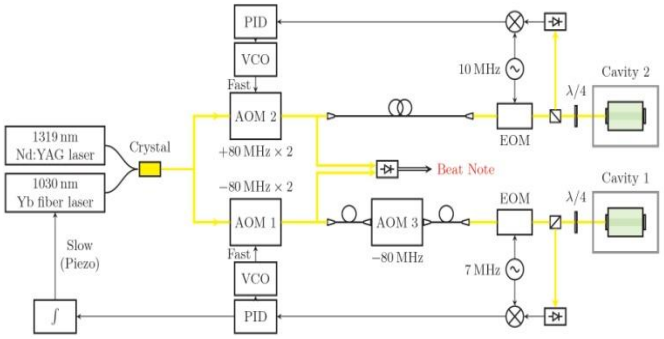

Figure 8. Scheme of the optical bench to lock the lasers on the two ultrastable cavities.EOM: Electro-Optic Modulator, AOM: Acusto-Optic Modulator, VCO: Voltage Controlled Oscillator, PID: Proportional-Integral-Derivative control.

The bandwidth of the control is 150 kHz, limited by the delay in the AOMs.

The PDH signal from the first cavity is also used for a slow lock on the piezoelectric actuator of one of the two infrared lasers to correct for their slow drift. A third AOM is then used at fixed frequency to bridge the frequency difference of the two cavities, and to allow for a contemporaneous lock of the two laser onto the two cavities.

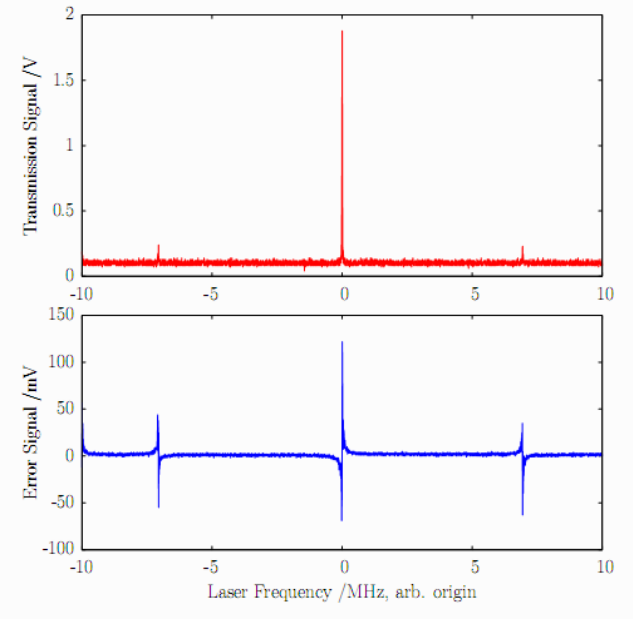

Figure 9. Pound-Drever-Hall signals from the cavities.

IV. LASER CHARACTERIZATION

The laser beams, stabilized against the two cavities, are extracted before the optical fibers delivering them to the anti-acoustic chambers and are superimposed on a fast photodiode. The resulting beat note is then filtered, amplified, down-converted and counted using a hydrogen maser as a reference. The noise of the two lasers is independent within the bandwidth of the two controls. The bandwidth is about 150 kHz as measured observing the spectrum of the beat note reported in Figure 10, obtained with a resolution bandwidth of 4.7 kHz, a span of 500 kHz, and a sweep time of 86 ms. A close up scan of the beat note allows to observe a Lorentzian line profile of (3.8 ± 0.1) Hz width that correspond to a single laser linewidth < 2 Hz, as shown in Figure 11, obtained with a resolution bandwidth of 3 Hz, a span of 500 Hz, and a sweep time of 617 ms.

Figures 12 and 13 respectively report the phase noise power spectral density and the overlapping Allan deviation of the beat note frequency.

The phase noise spectrum has been measured using a 40-divider to manage the high phase power at low frequencies. In Fig. 12, the lower curve is referred to the phase spectrum with the damping platform activated, while the upper one shows the spectrum when the damping platform is not activated. The baseline of the lower spectrum is fitted by the polynomial:

$$S_\varphi(f) = b_{-3}f^{-3} + b_{-2}f^{-2} + b_0. \qquad (1)$$

with $b_{-3} =$ 3.8 rad^{2}Hz^2, $b_{-2} = 0.05$ rad^{2}Hz, $b_0 = 3.5 \times 10^{-8}$ rad^{2}Hz^{-1}.

In the spectral range between 10 Hz and 1000 Hz is evident an excess of noise with respect to the fitting baseline.

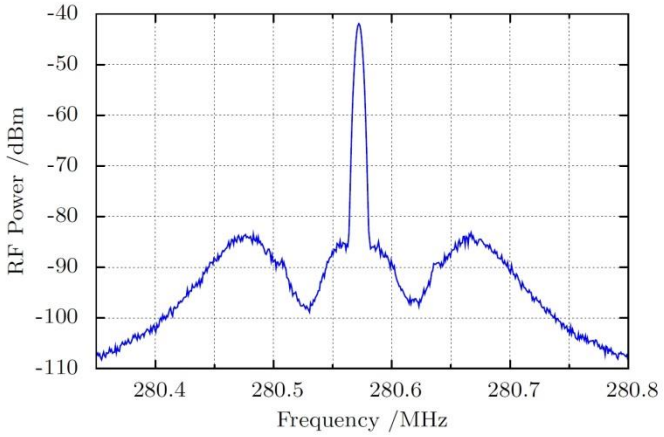

Figure 10. Beat note between the two independent locked lasers, (Resolution Bandwidth 4.7 kHz, Span 500 kHz, Sweep Time 86 ms). The control loop bandwidth is evaluated to be 150 kHz.

Considering the upper spectrum, without the vibrations damping by the platform, there is generally a noise increase in the 10-1000 Hz range, but in particular two peaks at 10 Hz and 20 Hz are observed, with a power of about 2×10^{-4} rad^2/Hz . These two peaks are caused by the seismic vibrations as reported in Fig.6, where the measured acceleration spectrum of the cavitiy box floor shows peaks at the same frequencies along the *x* and *y* directions. Using these peaks, the experimental vibration sensitivity of the cavities is measured to be about 3×10^{-10} s^2/m not the lowest possible as evaluated by the Finite Elements Analysis. The discrepancy is probably due to a displacement of the supporting pads position from the optimum by 1-2 mm, as discussed in the Section III.

The Allan deviation plots reported in Fig. 13 refer to the measurement without vibration damping (upper curve), with damping (lower curve, squares) and this latter with a linear drift removal on the data (lowest, circles).

The presence of the damping platform is outstanding for short integration time, and we have already commented about on the phase noise spectrum analysis.

The deviation shown for longer averaging time is consistent with a 0.8 Hz/s linear drift.

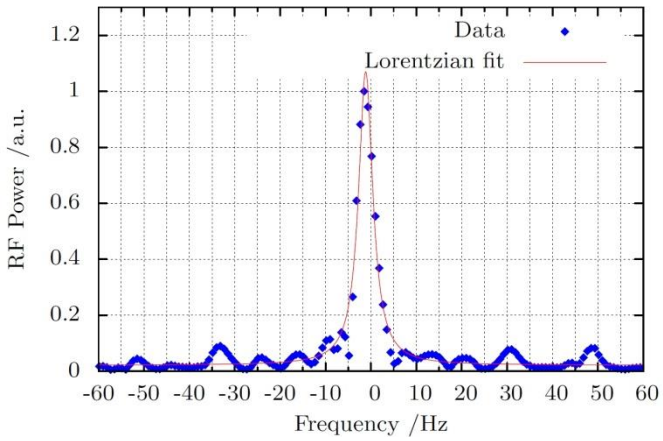

Figure 11. Beatnote between the two indipendent locked lasers, showing a linewidth of 3,8 Hz (Resolution Bandwidth 3 Hz, Span 500 Hz, Sweep Time 617 ms).

After the drift removal, the flicker floor of the beat note instability is 4×10−15, probably limited by amplitude to frequency noise conversion. This corresponds to an estimated stability for each laser of 2.8×10−15. It is worth notice that the amplitude noise in the laser is not in common mode, since derives from the fiber polarization noise and not from the yellow source. This flicker floor is clearly observed when a drift of 0.8 Hz/s is removed from the data. We evaluated the limit from the thermal noise σ_{Th}^2 in the ULE cavities using the equation reported in [7]:

$$\sigma_{Th}^2 = ln2\ \frac{8k_BT}{\pi^{\frac{3}{2}}}\frac{1-s^2}{Ew_0L^2}\left(\varphi_{sub} + \varphi_{coat}\frac{2}{\sqrt{\pi}}\frac{1-2s}{1-s}\frac{d}{w_0}\right) \qquad (2)$$

Here, k_B is the Boltzmann constant, T the mirror temperature, s and E are the Poisson's ratio and the Young's modulus of the ULE glass, L is the cavity length, $w_0$is the laser beam radius (1/e field) on the mirror, φ_{sub} and φ_{coat} are the mechanical losses for the mirror substrate and for the coating, and d is the thickness of the coating.

Considering in our case E=67.6×10^9 Pa, s=0.17, w_0=190 μm, L= 0.10 m, d=2 μm, φ_{sub}= 1.67×10^{-4} and φ_{coat}= 4×10^{-14} in the spectral range 100 Hz – 10 kHz , we obtain a flicker thermal limit instability of 8×10^{-16} for each cavity, and about 1×10^{-15} for the beatnote.

Another contribution to the flicker frequency noise in Fabry-Pérot stabilized laser is due to the optical power fluctuations resulting in a resonant frequency fluctuation of the cavity. This phenomenon may be caused by a coating absorption or a radiation pressure effect [8-10]. The frequency sensitivity $h(f)$ to absolute fluctuations of the power transmitted through the cavity, expressed in Hz/μW, in the low spectral region ($f \ll \Delta\nu_{cav}$) can be approximated as

$$h(f) = L^{-1}K_P F\nu_0 \qquad (3)$$

Here, K_P is a conversion parameter mainly determined by the features of the mirror and laser beam size, F and L the cavity finesse and length, $\nu_0$the laser frequency.

The power impinging the cavities is 60 μW, the transmitted power is 20% and its relative instability reproduces the performances of the source, as reported in Fig. 3; with a degradation that is conservatively evaluated in 2×10^{-3} for averaging time $\tau > 1$ s, that is three times the instability of the source. The power noise on the two cavities is uncorrelated. Considering the laser power,the dimensions of the two cavities and their finesses, the observed flicker floor instability of 4×10^{-15} is compatible with a frequency sensitivity $h(f) = 75$ Hz/μW and a conversion parameter $K_P = 5.8\times10^{-20}$ m/μW. This latter value is larger than the values reported in [8], but it is consistent with the value that we measured in another experiment based on two Fabry-Pérot cavities, resonating at 1550 nm, with the same geometry and materials of the cavities used in this work [11].

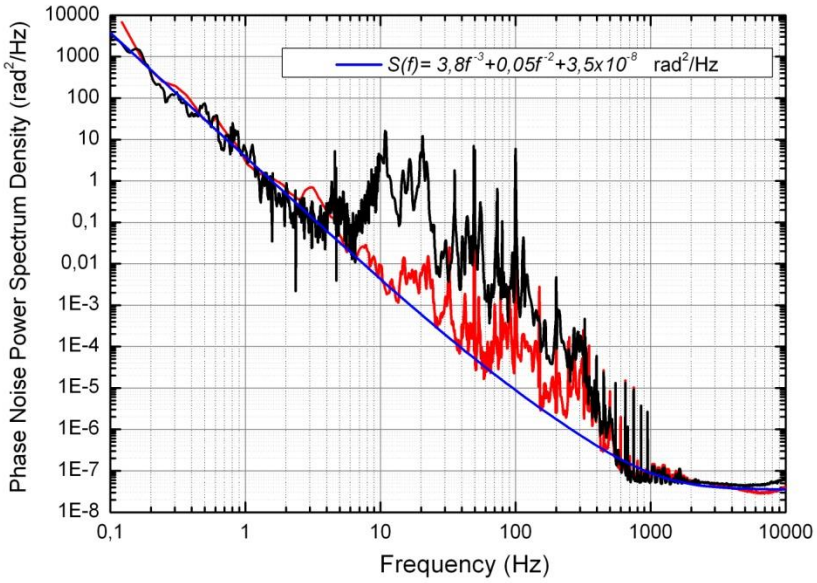

Figure 12. Phase noise power spectrum density of the beat note with and without seismic damping table activate. The original measurement has been taken with a phase 40-divider

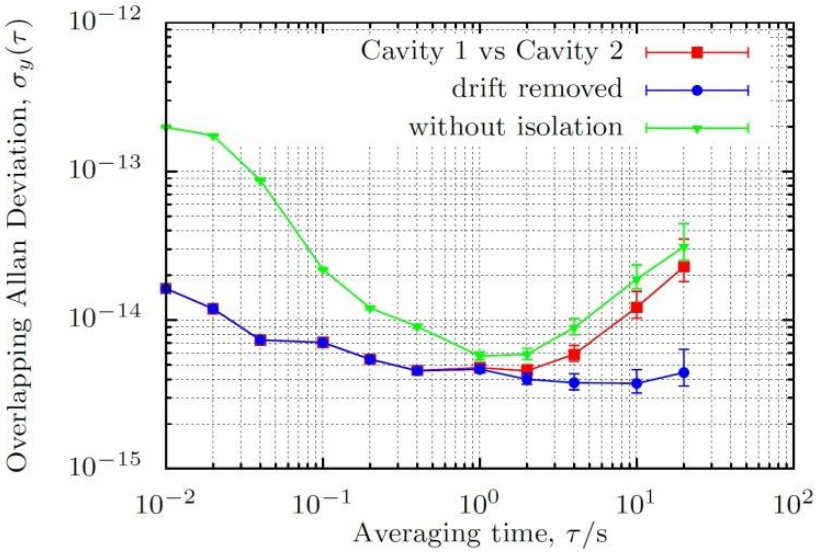

Figure 13. Allan deviation of the lasers beat note: with and without seismic damping table activate, with seismic damping and 0,8 Hz/s drift removal (blue).

CONCLUSIONS

We have described the generation and frequency stabilization of a 578 nm laser source to be used in a ytterbium optical clock realization. The source has been characterized and its relative frequency instability is presently 3×10^{-15} (flicker floor) corresponding to a linewitdth <2 Hz. The present realization is not limited by the seismic vibrations sensitivity or temperature fluctuations, while a limitation is provided by conversion from laser amplitude to frequency modulation. This limitation could be improved decreasing the laser power impinging the cavity or by its stabilization, to reach the thermal noise limit of 1×10^{-15}.

ACKNOLEDGEMENTS

The authors would like to acknowledge E. K. Bertacco for helping with electronics, C. Clivati for the useful discussions and M. Zucco and M. Bisi of INRIM's Length division for their help. We would also acknowledge the technical help of V. Fornero and of the INRIM machine workshop

This work is funded by: Regione Piemonte, YTRO contract.

REFERENCES

[1] N. D. Lemke, A. D. Ludlow, Z. W. Barber, T. M. Fortier, S. A. Diddams, Y. Jiang, S. R. Jefferts, T. P. Heavner, T. E. Parker, and C. W. Oates, "Spin ½ Optical Lattice Clock", Phys. Rev. Lett. 103, 063001, 2009.

[2] A.Yu. Nevsky et al., "A narrow-line-width external cavity quantum dot laser for high-resolution spectroscopy in the near-infrared and yellow spectral ranges", Appl Phys B, 92: 501, 2008

[3] C. W. Oates, "Stable Laser System for Probing the Clock Transition at 578 nm in Neutral Ytterbium", Frequency Control Symposium, 2007 Joint with the 21st European Frequency and Time Forum. IEEE International, Geneve, 29 May -1 June 2007, pp 1274

[4] K. Hosaka et al., "Evaluation of the clock laser for an Yb lattice clock using an optic fiber comb", IEEE Transactions on Ultrasonics, Ferroelectrics and Frequency Control, Vol 57, p 606, 2010

[5] T. Nazarova, F. Riehle, and U. Sterr, "Vibration insensitive reference cavity for an ultra-narrow-linewidth laser," Appl. Phys. B 83, 531–536 (2006).

[6] J. Millo, D. V. Magalh˜aes, C. Mandache, Y. L. Coq, E. M. L. English, P. G. Westergaard, J. Lodewyck, S. Bize, P. Lemonde, and G. Santarelli, "Ultrastable lasers based on vibration insensitive cavities," Phys.Rev. A 79, 053829 (2009).

[7] K. Numata, A. Kemery, and J. Camp, "Thermal-noise limit in the frequency stabilization of lasers with rigid cavities," Phys. Rev. Lett. 93, 250602–1–4 (2004).

[8] B. C. Young, F. C. Cruz, W. M. Itano, and J. C. Bergquist, "Visible lasers with subhertz linewidths,"Phys. Rev. Lett. 82, 3799–3802 (1999).

[9] Caves, C.M. "Quantum-mechanical radiation-pressure fluctuations in an interferometer" Phys. Rev. Lett., 45, 75–79 (1980)

[10] Dorsel, A., McCullen, J.D., Meystre, P., Vignes, E. & Walther, H. “Optical bistability and mirror confinement induced by radiation pressure” Phys. Rev. Lett., 51, 1550–1553 (1983)

[11] C. Clivati, et al., “Fiber Link with 1E-19 frequency stability using a Planar-Waveguide External Cavity Laser Diode”, submitted to IEEE-Trans. On UFFC